KAPILASHRAMI, A., GÖRNERUP, M., LAHIRI, A.K., and SEETHARAMAN, S. Foaming of model slags containing V_2O_5 under dynamic conditions. *V II International Conference on Molten Slags Fluxes and Salts*, The South African Institute of Mining and Metallurgy, 2004.

Foaming of model slags containing V_2O_5 under dynamic conditions

A. KAPILASHRAMI*, M. GÖRNERUP*, A.K. LAHIRI†, and S. SEETHARAMAN*
**KTH Material Science and Engineering, KTH, Stockholm, Sweden*
†Department of Metallurgy, Indian Institute of Science, Bangalore, India

Simultaneous reduction and foaming of chromium-rich slag have been studied in a laboratory furnace equipped with X-ray image analysis. Reduction of the metal oxides by graphite generated CO, which caused the melt to foam. The slag composition continuously changed due to reactions and dissolution of lining. Gas generation rate, foam height, and gas bubble size were studied and correlated to slag composition.

Viscosity increased significantly during the experiments due to a change in slag composition. Bubble sizes varied little during the progress of reactions but differed considerably for different slags. Bubble sizes were largest for V_2O_5 containing slag, which is contrary to the general understanding that the presence of strong surface active agents reduces the bubble size. The foaming index did not follow expected trends for bubble size and viscosity, suggesting that foaming index is not a suitable parameter for discussion of foams under dynamic conditions.

Keywords: slag, foaming, dynamic conditions

Introduction

Foaming is a common feature in all steelmaking processes. Recently Lahiri *et al.*[1] pointed out that almost all the oxides present in steelmaking slag are surface active, which gives rise to foaming. In the electric arc furnace processes (EAF), the foam protects the vessel from arc radiation and stabilizes the arc, thus enabling higher production rates. However, excess foam becomes undesirable. It is therefore important to understand the factors responsible for proper foam growth and the methods to control foaming in steelmaking processes.

Earlier studies have mostly concerned the foaming behaviour of slag at steady-state where foam is generated by bubbling gas through a nozzle. Attempts to rationalize the foaming behaviour have been made by introducing the foaming index[2,3] which correlates the foam height H with the superficial gas velocity U:

$$\sum = \frac{H}{U} \qquad [1]$$

The foaming index has been empirically related to surface tension σ, viscosity μ, density ρ of the liquid, and the size of the bubbles d_b[4–6]. Consensus has, however, not been reached on the magnitude of the influence of these parameters on the foaming index. Zhang and Fruehan[4] have, for different slags, shown that the foaming index can be represented as

$$\sum = \frac{115\mu^{1.2}}{\sigma^{0.2}\rho d_b^{0.9}} \qquad [2]$$

while Kim *et al.*[5] showed that $CaO\text{-}SiO_2\text{-}FeO$ and $CaO\text{-}SiO_2\text{-}FeO\text{-}MgO\text{-}X$ systems ($X=Al_2O_3$, MnO, P_2O_5 and CaF_2) follow the relationship

$$\sum = \frac{C\mu}{(\sigma\rho)^{0.5}} \qquad [3]$$

where C depends on the nature of the slag. Lahiri and Seetharaman[7] discussed the above empirical equations of the foaming index and showed that the foaming index for a foam of uniform bubbles can be expressed as

$$\sum = \frac{C\mu}{\rho d_b} \qquad [4]$$

During steelmaking, slag composition changes continuously because of oxidation and reduction reactions and the dissolution of flux and lining. The change in slag composition for alloy steelmaking is more complex because of the presence of oxides like Cr_2O_3 and V_2O_5 in slag phase. Besides the change in slag composition, the gas generation rate depends on the oxidation rate of carbon, and it varies significantly with the progress of the process. It is not yet known if the foaming index concept is directly applicable to this situation.

The aim of the present work is to study the foaming behaviour under dynamic conditions. Typical slag compositions found in the production of stainless steel and tool steel in EAF have been employed.

Experimental

The experimental set-up and measurement procedure is described in detail elsewhere[8]. Pre-melted slag samples were placed in a crucible (id.= 40 mm) with graphite bottom and alumina-lined sides. The crucible was placed in a furnace with constant temperature (± 5 K) and was continuously flushed with argon gas. The experiments were carried out at 1923 K. The slag behaviour was recorded on VHS through X-ray equipment connected to a CCD

camera. Samples were regularly taken for chemical analysis. The VHS recordings were used for evaluation of the foam behaviour.

A synthetically produced slag with typical compositions found in tool and stainless steelmaking processes was used. Table I shows the initial compositions of the different slags. The parameters varied were V_2O_5 content and basicity of the slag. Basicity is here defined as

$$B = \frac{\%(CaO)}{\%(SiO_2)} \quad [5]$$

Results and discussion

When heated to melting temperatures, the metal oxides of the slag were reduced by the graphite, resulting in CO gas generation. The system is dynamic with continuous change in composition, as is the case in industrial processes. The change in chemical composition was measured with time and the gas generation rates were calculated from this.

Viscosity

The viscosity of the slag melt was calculated using a model based on the optical basicity Λ of the compounds[9]. The viscosity is calculated from

$$\ln \eta = \ln A + \frac{B}{T} \quad [6]$$

where A and B are constants derived from the corrected optical basicity, Λ_{corr}, of the system which is calculated from

$$\wedge^{corr} = \frac{\sum x_i n_i \Lambda_i}{\sum x_i n_i} \quad [7]$$

n_i, x_i being the number of oxygen atoms and the mole fraction of molecule i, respectively. Instead of using standard values found in literature, Mills et Sridhar[9] employed curve-fitted values of Λ_i. Curve-fitted Λ_i values of Cr_2O_3 and V_2O_5 are yet not available and these were therefore approximated with values for Fe_2O_3 and P_2O_5, respectively. The expression for the corrected optical basicity is similar to the regular expression for optical basicity. A correction in cation concentration has been made to charge balance the Al^{3+} ions that are incorporated in the silicate network by subtracting the appropriate amount required for charge balance from the concentration of CaO.

Figure 1a shows that viscosity initially decreases followed by an increase with time. The largest increase is found for the slag with 5% V_2O_5. The changes in composition show a corresponding large increase in alumina (Figure 1b), due to dissolution of the Al_2O_3 lining of the crucible. The dissolution of Al_2O_3 is greater at higher basicity but resulted in a comparatively lower increase in viscosity.

Comparisons with $CaO\text{-}SiO_2\text{-}FeO_x\text{-}Al_2O_3$ systems show that an increase in viscosity with increasing alumina content is expected[10]. Figure 1a further shows that Al_2O_3 dissolution increases with increasing V_2O_5 content. At present, the reason for higher dissolution of Al_2O_3 in the V_2O_5 containing slag cannot be stated with certainty, but larger contact area with the alumina lining due to higher foam height appears to be one factor.

Even though the alumina content increases monotonically in the samples from the beginning of the measurements, the viscosity of the melts decreases in the first twenty minutes or so. This decrease can be linked to the decrease in concentration of Cr_2O_3 and also FeO.

Bubble size

Figure 2 shows bubbles from Slag A and C at t = 22 min and t = 5 min, respectively, from the start of the reaction. The bubble sizes changed during the progress of the reaction. The bubble sizes fluctuated within ± 1 mm but no trend could be established in the fluctuations. The range of bubble sizes is listed in Table II. During the reaction, there was a significant change in gas generation rate as well as the viscosity of the slag due to reduction of FeO, Cr_2O_3 and

Table I
Initial composition of the slags used

	B	%Al_2O_3	%FeO	%MgO	%Cr_2O_3	%MnO	%V_2O_5
Slag A	1.5	7	5	5	10	2	0
Slag B	1.0	7	5	5	10	2	0
Slag C	1.5	7	5	5	5	2	2
Slag D	1.5	7	5	5	5	2	5

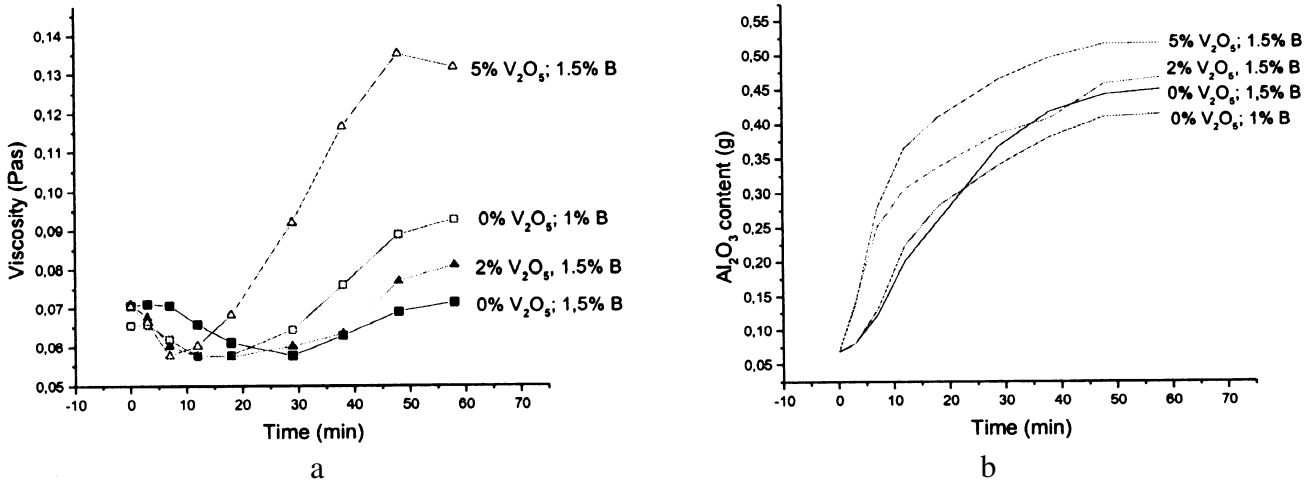

Figure 1. Variation of (a) viscosity and (b) Al_2O_3 content of slag with time

V_2O_5 and dissolution of Al_2O_3 but this did not lead to changes in bubble size. It is well known that when bubbles are formed by gas injection through a nozzle with a gas flow rate corresponding to a Reynolds number less than 500, bubble size is independent of gas flow rate and viscosity of liquid. It appears that a similar situation holds good for the present case. Ogawa *et al.* presented a model[11] according to which the critical bubble size formed from gas generation should increase with the increase of the surface tension of slag. Estimations show that the variation of surface tension is expected to be less than 10%. Hence, the effect may not be noticeable in the present case.

The bubble sizes are, however, found to differ significantly for different slag chemistries (Table II). The bubbles increase slightly with decreased basicity. The increase in bubble size with V_2O_5 content is notable. The decrease in surface tension when going from 5 mass % (i.e. 1.8 mole % in our system) to 0% in the systems $CaO-SiO_2-V_2O_5$ and $Al_2O_3-CaO-MgO-SiO_2-V_2O_5$ are 9% and 13%, respectively[10]. Since V_2O_5 decreases surface tension of the slag, the bubble sizes are expected to become smaller according to Ogawa's model. The results of Ogawa *et al.* were, however, based on force balances and are strictly valid for zero gas flow rate. Hence, the results may not be valid under the present conditions.

It is known that Marangoni force can produce smaller bubbles[12] but the cause for the observed larger bubble size is not clear. One possible reason could be that the area over which the bubble grows is higher in the presence of V_2O_5. We know that when a bubble grows at the tip of a nozzle, at low Reynolds numbers, the bubble diameter is given by

$$d_b = \left(\frac{6\sigma d_n}{\rho g} \right)^{1/3} \quad [8]$$

If the area over which the bubble grows is taken as equivalent to the nozzle area in Equation [8], larger bubble diameters will result from a larger bubble growth area.

Foaming index

The nature of foam formed from gas generation can be classified into true foam and dispersed phase (Figure 2). Initially the foam is of the dispersed phase type for slags without V_2O_5, but once the gas generation rate becomes high, it turns into true foam. For slags containing V_2O_5, i.e. Slags C and D, the foam is always of the dispersed phase type. The foaming index is in fact only meaningful for two-phase foam where both bubble dispersed phase and true foam are present[7]. Thus, the foaming index may not be directly applicable in the case of this study but can nevertheless be employed for a qualitative discussion.

Figure 3 shows the variation of the foaming index with time. In spite of the scatter of data points, all the curves indicate that the foaming index goes through a maximum. Comparison with the gas generation data indicates that the maxima in the foaming index correspond to a minimum gas generation rate. Secondly, the results show that there is no correlation between foaming index and slag viscosities. The average foaming index of different slags follows the trend C < A < B < D while the bubble size changes as A < B < C < D. According to Equations [2] and [4], the foaming index is inversely proportional to bubble diameter. Obviously the present result is not in agreement with it.

Foam height

Comparison of Figure 4a and b shows that the foam height is influenced by the gas generation rate, but there is not a 1:1 correspondence between the two. This is clear during the first 20–30 minutes. An increase in the gas generation

Table II
Size range of bubbles found in the different slags

	A	B	C	D
Average bubble size	4–5.5 mm	5.5–7.3 mm	7.5–9.3 mm	10–11 mm

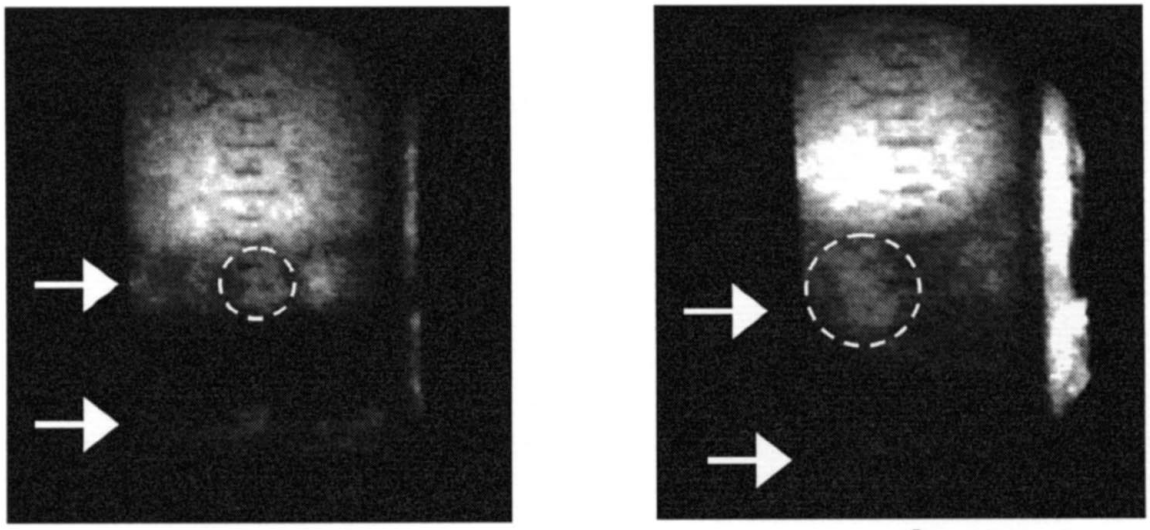

a b

Figure 2. X-ray images of two slag melts. The arrows point out the foamy layer and the crucible bottom , and the dashed circles indicate bubbles. (a) Slag A has a true foam layer at the top. Bubbles can be seen forming at the graphite. (b) The foamy layer of Slag C is of a dispersed phase type

rate increases the foam height but when the gas generation drops, the foam height remains a while before it decreases. The delay can be due to high viscosity of the melt. As the viscosity increases, the response delay increases. After 30 minutes, the foam height is practically unaffected by the change in gas generation rate, which could be due to the slow response of the system at high viscosities.

Conclusion

The nature of foam was found to be dependent on the slag chemistry.

During the progress of the reaction, the viscosity of all the slag melts decreased, initially due to the reduction of oxides, followed by an increase due to dissolution of the alumina lining. The bubble size was constant throughout the reaction in a slag but differed considerably among the different slags. V_2O_5 promoted the formation of large bubbles, which is notable since decreased surface tension should result in a decrease in bubble size. This phenomenon might be due to an increase in bubble growth area.

The foaming index did not show any dependence on either bubble size or viscosity. The foaming index is not a suitable parameter, even for qualitative discussion of foams under dynamic conditions.

The foam height is affected by the gas flow rate but the response is not immediate. The viscosity of the slag causes a delay in the change of foam height, with respect to the gas flow rate.

References

1. LAHIRI, A.K., YOGHAMBA, R., DAYAL, P., and SEETHARAMAN, S. *Proc. Mills symposium: Metals, slags, glasses: High temperature properties and phenomena*; Aune, R.E., and Sridhar S. (eds.). Institute of metals, London, 22–23 August 2002, vol. 1, pp. 231–238.
2. ITO, K., and. FRUEHAN, R.J. *Metall. Trans. B*, vol. 20B, 1989, pp. 509–514.
3. ITO, K. and FRUEHAN, R.J. *Metall. Trans. B*, vol. 20B, 1989, pp. 515.
4. ZHANG, Y. and FRUEHAN, R.J. Metall. *Mater. Trans. B*, vol. 26B, 1995, pp. 803–812.
5. KIM, H.S., MIN, D.J., and PARK, J.H. *ISIJ Int.*, vol. 41, no. 4, 2001, pp. 317–323.
6. JUNG, S. and FRUEHAN, R.J. *ISIJ Int.*, vol. 40, 2003, pp. 348–355.
7. LAHIRI, A.K., and SEETHARAMAN, S. *Metall. Mater. Trans. B*, vol. 33B, 2002, pp. 499–502.
8. DIVAKAR, M., GÖRNERUP, M., and LAHIRI, A.K. *Ironmaking Steelmaking*, vol. 29, no. 4, 2002, pp. 297–302.
9. MILLS, K.C., and SRIDHAR, S. *Ironmaking Steelmaking*, vol. 26, no. 2, 1999, pp. 262–268.
10. *Slag Atlas*, 2nd edn., VDEh, Verlag Stahleisen GmbH, 1995.
11. OGAWA, Y., HUIN, D., GAYE, H., and TOKUMITSU, N. *ISIJ Int.*, vol. 33, no. 1 , 1993, pp. 224–232.
12. MUKAI, K. *CAMP-ISIJ*, vol. 1, 1988, p. 260.

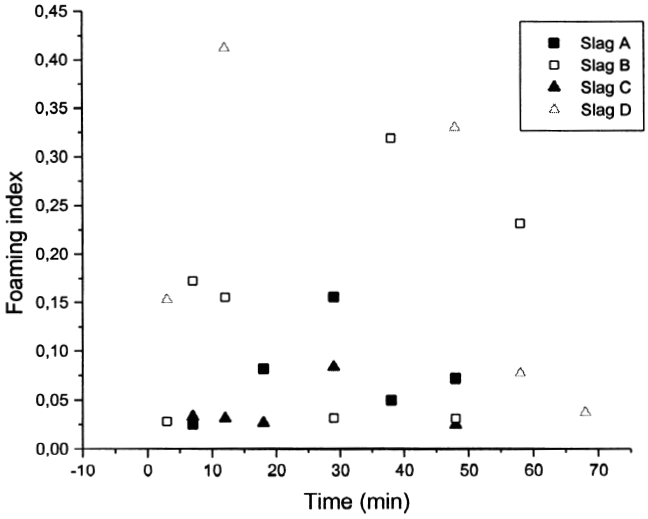

Figure 3. Foaming index of the samples over time, calculated according to Equation [1]. The average bubble sizes of the samples are indicated in the graph label

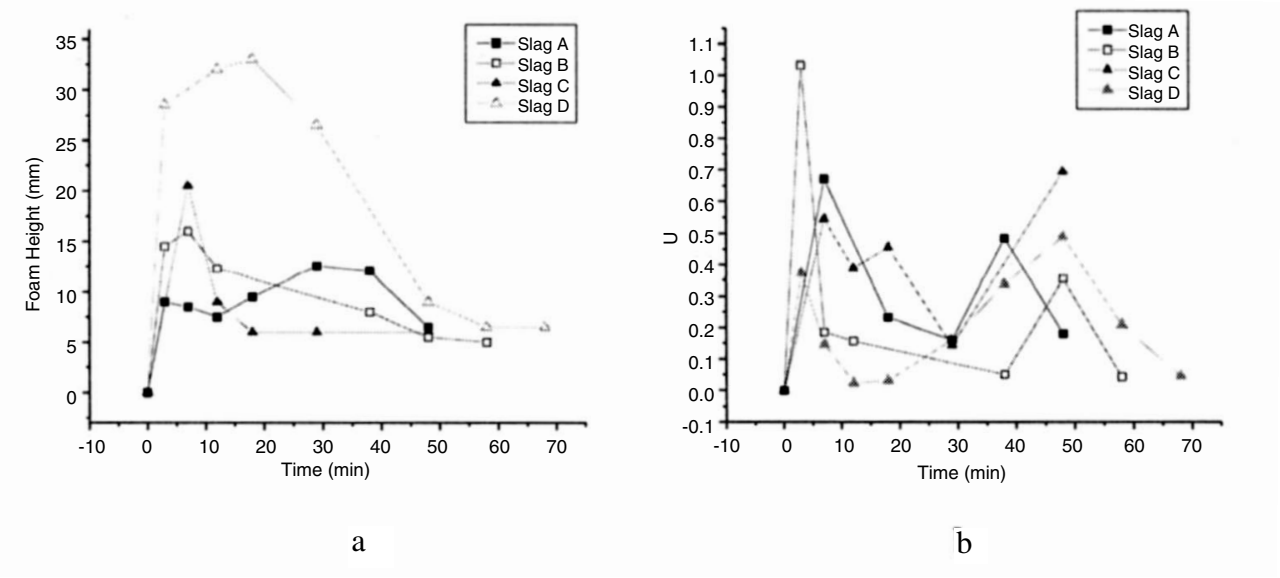

Figure 4. Variation of (a) foam height and (b) the gas generation with time